Protein Engineering, Design & Selection vol. 19 no. 5 pp. 205–210, 2006
Published online March 3, 2006 doi:10.1093/protein/gzl002

Mapping of residues involved in the interaction between the *Bacillus subtilis* xylanase A and proteinaceous wheat xylanase inhibitors

J.F.Sørensen[1,3] and O.Sibbesen[2]

[1]Danisco, Edwin Rahrs Vej 38, DK-8220 Brabrand and [2]Danisco, Langebrogade 1, DK-1001 Copenhagen C, Denmark

[3]To whom correspondence should be addressed.
E-mail: jens.frisbak.sorensen@danisco.com

The *Bacillus subtilis* xylanase A was subjected to site-directed mutagenesis, aimed at changing the interaction with *Triticum aestivum* xylanase inhibitor, the only wheat endogenous proteinaceous xylanase inhibitor interacting with this xylanase. The published structure of *Bacillus circulans* XynA was used to target amino acids surrounding the active site cleft of *B.subtilis* XynA for mutation. Twenty-two residues were mutated, resulting in 62 different variants. The catalytic activity of active mutants ranged from 563 to 5635 XU/mg and the interaction with *T.aestivum* xylanase inhibitor showed a similar variation. The results indicate that *T.aestivum* xylanase inhibitor interacts with several amino acid residues surrounding the active site of the enzyme. Three different amino acid substitutions in one particular residue (D11) completely abolished the interaction between *T.aestivum* xylanase inhibitor and *B.subtilis* xylanase A.

Keywords: endo-β-1,4-xylanase/inhibition/site-directed mutagenesis/TAXI/XIP

Introduction

Endo-1,4-β-xylanases (EC 3.2.1.8), first reported in 1955 (Whistler and Masek, 1955), catalyze the hydrolysis of the 1,4-β-xylanosidic linkage in xylan, one of the most abundant plant cell wall polysaccharides in nature. Arabinoxylans are often highly complex polysaccharides (Fincher and Stone, 1986). The 1,4-β-xylopyranosidic backbone may be acetylated and modified by the addition of α-4-*O*-methylglucoronic acid or α-arabinofuranose. p-Coumaric acid or ferulic acid may additionally be linked to the α-arabinofuranose moiety.

Based on structural and genetic information, xylanases have been classified into different glycoside hydrolase families (GHs) (Henrissat, 1991; Coutinho and Henrissat, 1999). Until recently, all known and characterized xylanases belonged to the families GH10 or GH11. Recent work has identified numerous other types of xylanases belonging to the families GH5, GH7, GH8 and GH43 (Coutinho and Henrissat, 1999; Collins *et al*., 2005). Until now the GH11 family differs from all other GHs, being the only family solely consisting of xylan-specific xylanases.

Hitherto, three types of proteinaceous xylanase inhibitors endogenously present in cereals have been described. The first type described was the TAXI-type (*Triticum aestivum* xylanase inhibitor) inhibitor (Debyser *et al*., 1997; Rouau and Surget, 1998; Sibbesen and Sørensen, 1998). TAXI-type inhibitors are proteins of ∼40 kDa and pI values of 8.7–9.3. Based on amino acid sequence and specificity, TAXI-type inhibitors can be subdivided into TAXI-I and TAXI-II (Gebruers *et al*., 2001). Available data indicate that TAXI-type inhibitors are specific for GH11 xylanases (Furniss *et al*., 2002; Brutus *et al*., 2004; Gebruers *et al*., 2004a; Beliën *et al*., 2005). Published structures of TAXI-I (Sansen *et al*. 2004a) and TAXI-I in complex with *Aspergillus niger* xylanase 1 (AnX) (Sansen *et al*., 2004b) are available. The second type of inhibitors to be characterized was the XIP-type (xylanase inhibitor protein) (McLauchlan *et al*., 1999). These inhibitors are proteins of ∼29 kDa and pI values of 8.7–8.9. Flatman *et al*. (2002) showed that the XIP-type specificity differs from TAXI-type specificity, the XIP-type being able to inhibit both GH10 and GH11 xylanases. The basis for XIP's dual specificity has recently been identified as two independent binding sites for GH10 and GH11 xylanases respectively (Payan *et al*., 2004). XIP-type inhibitors have been reported to inhibit only GH11 xylanases of fungal origin, leaving bacterial GH11 xylanases unaffected (Juge *et al*., 2004). A distinction between bacterial and fungal GH11 xylanases can hardly be justified from a protein structural standpoint and fungal GH11 xylanases unaffected by XIP have indeed been identified recently (Beliën *et al*., 2005). The third type of inhibitors is named TL-XI (thaumatin-like xylanase inhibitors). This type has been discovered recently and is still only partially characterized (Gebruers *et al*., 2004b).

Due to the abundance of xylan in plant cell walls, xylanases are widely used commercially as improvers and processing aids in plant based industries such as industrial baking (Maat *et al*., 1992; Rouau *et al*., 1994; Courtin and Delcour, 2002), gluten–starch separation (Christophersen *et al*., 1997), animal feed (Bedford and Classen, 1992) and paper manufacturing (Viikari *et al*., 1986). The efficiency of commercially available xylanases is therefore of considerable economical interest and the presence of endogenous xylanase inhibitors in plants is likely to be the single most important factor hampering the enzymatic process. We therefore took on the challenge to modify a xylanase in order to diminish the xylanase–inhibitor interaction, preferably without interfering with the catalytic properties of the xylanase.

Site-directed mutagenesis has been used extensively in the study of xylanases. Since Wakarchuk *et al*. (1994) confirmed the identification of the catalytic residues in *Bacillus circulans* xylanase A by mutational analysis, the catalytic activity (Moreau *et al*., 1994), the substrate binding (Wakarchuk *et al*., 1994; Ponyi *et al*., 2000; de Lemos Esteves *et al*., 2004) and the pH optimum (Joshi *et al*., 2000; Liu *et al*., 2004) has been studied and modified by changing specific amino acid residues. Reports on the modification of the xylanase–inhibitor interaction by changing the xylanase have also appeared in the literature (Tahir *et al*., 2002, 2004). The latter studies showed that the interactions between XIP

or TAXI and AnX could be eliminated by the mutations N117A (XIP interaction) or D37A (XIP and TAXI interaction) in AnX. However, the catalytic activity of the uninhibited D37A variant of AnX was severely hampered by the mutation. Thus, this variant is interesting from a scientific point of view but unlikely to become an industrially useful enzyme.

In the following, we describe the strategy and work leading to GH11 xylanases unaffected by any inhibitors from wheat, while still maintaining sufficient catalytic activity to be interesting candidates for commercial production. Using *Bacillus subtilis* xylanase A (Paice *et al*., 1986) (hereafter BsX) as template and a xylanase inhibitor preparation from wheat as screening tool, we have used a rational site-directed mutagenesis strategy to identify a set of surface residues surrounding the active site cleft involved in the BsX-inhibitor interaction. We hereby report on the relative importance of a set of residues for the interaction between BsX and TAXI. Among the variants described are xylanases being insensitive to all known wheat xylanase inhibitors.

Experimental procedures

Experimental strategy

BsX was chosen as the template for site-directed mutation as BsX is unaffected by XIP and TL-XI but not by TAXIs. As the presence of inhibitors other than TAXI affecting BsX cannot be ruled out in wheat, a crude wheat flour preparation was used for assaying the inhibition. As we wanted to avoid affecting the catalytic activity of the enzyme, amino acid residues participating in catalysis or situated inside the active site cleft have not been mutated. Instead, surface residues surrounding the cleft have been the targets for mutagenesis. An initial set of residues at the rim of the cleft was selected and based on the results obtained from this set, additional residues further away from the active site rim were selected.

Xylanases (EC 3.2.1.8)

BsX endo-β-1,4-xylanase (Swiss Prot entry: P18429) was used as a template for site directed mutagenesis. AnX endo-β-1,4-xylanase (Swiss Prot entry P55329) was used for the analysis of the XIP sample. The structure of *B.circulans* endo-β-1,4-xylanase (Swiss Prot entry P09850 and PDB ID: 1XNB) was used to target amino acids in BsX for mutation. The two molecules are identical, except for residue 147 situated on the opposite side of the area of interest in this study. S147 in BsX corresponds to T147 in the *B.circulans* xylanase (Figure 1).

The three-dimensional structure of GH11 xylanases resembles the shape of an open right hand. One sheet resembles the thumb and four sheets resemble the other four fingers. For BsX we have defined the residues making up the thumb as T109 to Y128 and finger 1 (index finger) as N54 to T67, finger 2 A170 to T183, finger 3 N25 to G39 and finger 4 W6 to N22 (Figure 1). The active site is made up by the cleft between the thumb and the four fingers where the catalytic residues are situated. For BsX these are E78 and E178 (Wakarchuk *et al*., 1994).

Molecule structures

Coordinates for the structures of *B.circulans* xylanase A (PDB ID: 1XNB) (Campbell *et al*., 1993) and the TAXI–AnX complex (PDB ID: 1T6G) (Sansen *et al*., 2004b) were downloaded from the RCSB Protein Data Bank (www.rcsb.org/pdb).

Software

Molecule structures were visualized by the use of Swiss-pdbviewer (GlaxoSmithKline, Middlesex, UK). Pictures shown were generated by using Swiss-pdbviewer in combination with 'PovRayTM for Windows' (www.povray.org). IC50 values were calculated by the use of GraphPad Prism software (GraphPad Software, Inc., San Diego, USA).

Xylanase mutation and production

Initially, the overlapping extension PCR method was used for mutagenesis and the resultant variant genes were expressed by the use of the pET24a vector and *Escherichia coli* BL21 system according to the manual provided by the vendor (Novagen, Madison, USA). A more convenient system was quickly adopted: A construct comprising the ribosome binding site from pET24a (ctagaaataattttgtttaactttaagaaggagatatacat) fused to the wild-type xylanase gene without signal sequence (atggctagcacagactactggcaa--------tggtaa) was transferred to the vector pCRBlunt (InVitrogen, Carlsbad, CA, USA). This resulted in constitutive expression of xylanase in TOP10 cells (InVitrogen) after transformation with the constructed vector, provided that the orientation of the gene is in a 'clockwise' direction. Site directed mutation in the gene was then obtained by the use of the 'QuickChange' mutagenesis kit (Stratagene, La Jolla, CA, USA) according to the manufacturer's protocol. Mutants were verified by sequencing. Sufficient production of the verified mutants was obtained by growing the transformed TOP10 cells in 1 L scale.

Xylanase purification

Escherichia coli TOP10 cells having expressed the xylanase were harvested by centrifugation (20 min, 3500 *g*, 20°C) and resuspended in 50 mM Tris, 2 mM EDTA, pH 7.4. Cells were opened by addition of 1 mg/ml lysozyme (ICN Biomedicals, Costa Mesa, CA, US, cat. No. 100831), stirring of the slurry for 2 h at ambient temperature, freezing and thawing followed by sonication. pH was adjusted to 4.0 using 1 M HCl followed by centrifugation (20 min, 3500 *g*, 20°C). The supernatant containing the xylanase was desalted using disposable PD-10 desalting columns (Amersham Bioscience, Sweden) equilibrated in and eluted with 50 mM sodium acetate, pH 4.5. The desalted sample was loaded onto a 10 ml SOURCE 15S column (Amersham Bioscience, Sweden) pre-equilibrated with 50 mM sodium acetate, pH 4.5. The column was then washed with equilibration buffer and eluted with a linear NaCl gradient (50 mM sodium acetate, 0–0.35 M NaCl, pH 4.5). Fractions containing xylanase activity were pooled and used for further analysis.

Xylanase assay

Samples were diluted in citric acid (0.1 M) di-sodium-hydrogen phosphate (0.2 M) buffer, pH 5.0, to obtain approximately OD_{590} = 0.7 in this assay. Three different dilutions of the sample were pre-incubated for 5 min at 40°C. At 5 min, 1 Xylazyme tablet (crosslinked, dyed xylan substrate, Megazyme, Bray, Ireland) was added to the enzyme solution in a reaction volume of 1 ml. At 15 min the

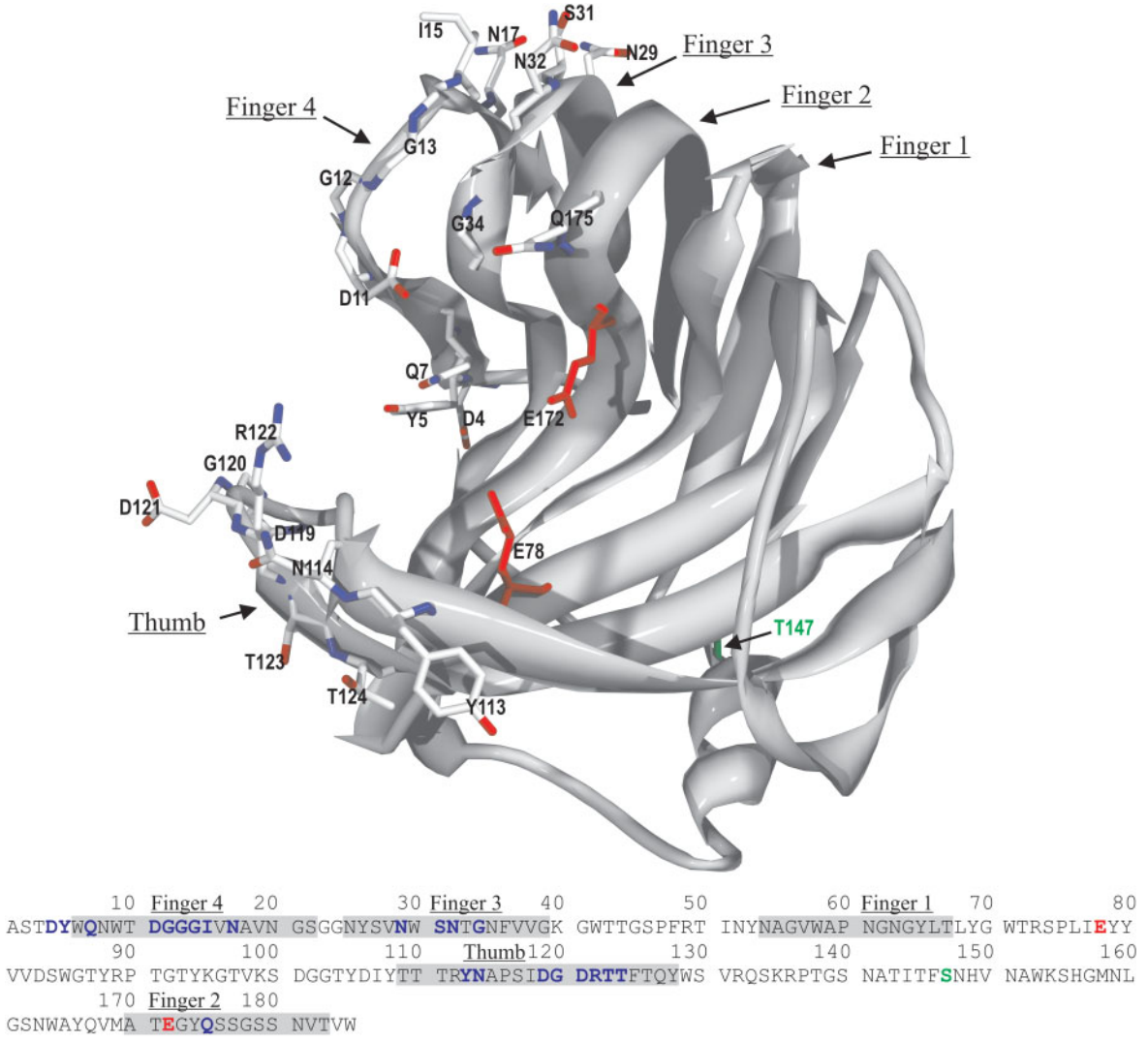

Fig. 1. Ribbon model of *B.subtilis* XynA (BsX) with surface residues targeted for site directed mutagenesis shown in CPK colors (Corey and Pauling, 1953; Koltun, 1965). The two catalytic glutamic acid residues are highlighted in red. The residue highlighted in green (T147) is threonine in *B.circulans* xylanase, but serine (S147) in BsX. The amino acid sequence of BsX (Paice *et al*., 1986) is inserted, thumb and fingers are indicated. The residues targeted for site-directed mutation are highlighted in bold/blue, the catalytic residues in bold/red and S147 in bold/green.

reaction was terminated by adding 10 ml of 2% Tris/NaOH, pH 12. Blanks were prepared using 1000 µl buffer instead of enzyme solution. The reaction mixture was centrifuged (1500 *g*, 10 min, 20°C) and the OD of the supernatant was measured at 590 nm. One xylanase unit (XU) is defined as the xylanase activity increasing OD_{590} with 0.1/min.

Specific activity determination

Optical density at 280 nm of the purified samples was measured for determining xylanase protein concentration. A theoretically calculated, specific OD_{280} (Gasteiger *et al*., 2003) of 0.25 U/mg × ml was used for the specific activity calculation. Xylanase activity was determined as described above.

Xylanase inhibition assay

One hundred microliters of inhibitor preparation, 250 µl xylanase solution (containing 2.2 XU xylanase/ml) and 650 µl buffer [0.1 M citric acid and 0.2 M di-sodium hydrogen phosphate buffer, 1% BSA (Sigma-Aldrich, USA), pH 5.0] was mixed. The mixture was thermostated for 5 min at 40.0°C. At 5 min one Xylazyme tablet was added. At 15 min reaction was terminated by adding 10 ml 2% Tris/NaOH, pH 12. The reaction mixture was centrifuged (1500 *g*, 10 min, 20°C) and the supernatant measured at 590 nm. The xylanase inhibition was calculated as residual activity in percent, compared with the blank. Blanks were prepared the same way, but substituting the inhibitor solution with water. A K_i value cannot be calculated using data from assays containing an insoluble substrate and a soluble inhibitor. In order to compare the variants, we have used a range of inhibitor preparation concentrations and measured the activity in the assay in percent of activity without inhibitor. The results were used for calculating an IC50 value (specific to this particular assay) of the variants by using the one site competition graph fitting mode in 'GraphPad' software. The equation used is the following:

$$Y = \frac{(\text{min.Value}) + ((\text{max.Value}) - (\text{min.Value}))}{(1 + 10^{(X - \text{LogIC50})})}$$

The obtained IC50 values are used for quantifying the change in inhibitor sensitivity caused by the mutation.

Inhibitor preparation

A crude inhibitor preparation (containing both TAXI and XIP, hereafter referred to as inhibitor preparation) was prepared from 1 kg wheat (*T.aestivum*) flour. The inhibitor preparation was extracted from the flour using water in a 1 : 3 ratio (w/w) followed by centrifugation (3500 *g*, 20 min, 4°C). The extract was kept at 65°C for 40 min, centrifuged (3500 *g*, 20 min, 4°C) and desalted using disposable PD-10 desalting columns (Amersham Bioscience, Sweden) pre-equilibrated with 20 mM sodium phosphate buffer, pH 7. TAXI concentration in the inhibitor preparation was determined by its inhibition of BsX. The protocol for purification and quantification of TAXI is described elsewhere (Sibbesen and Sørensen, 2001). XIP was purified to homogeneity as described elsewhere (Flatman *et al*., 2002).

Effect of pH on xylanase–inhibitor interaction

Assays were performed as described under xylanase assay and xylanase inhibitor assay, however, under different pHs ranging from 3.5 to 8.5. Buffer systems determining the pH were prepared by varying the citric acid (0.1 M) and di-sodium-hydrogen phosphate (0.2 M) ratios.

Results

Inhibition of BsX

The effect of the inhibitor preparation and a pure XIP preparation on BsX and AnX is illustrated in Figure 2. It is evident that BsX is unaffected by XIP.

Influence of pH on BsX–inhibitor interaction

The effect of pH on the interaction between the xylanase and inhibitor was studied. The interaction is strongly dependent on pH, indicative of electrostatic forces participating in the interaction. The pH profile of inhibition closely resembles the pH profile of the activity of the enzyme. This may indicate that some residues are important for substrate binding as well as for inhibitor binding (Figure 3).

Xylanase expression and purification

Twenty-two surface residues were target for site directed mutagenesis (Figure 1). Each residue was substituted by one or several amino acids. In this way 62 variants of BsX, each containing one point mutation were designed. Fifty-seven of the 62 variants were expressed as active xylanase in *E.coli*. Purified xylanase variants were obtained in yields ranging from 1.45 to 28.55 mg/l.

Specific activity of xylanase variants

Among the catalytically active variants the specific activity varies between 563 and 5635 XU/mg (D11K and Q175L, respectively). Wild-type BsX specific activity was determined to be 4162 XU/mg. Surface mutations can thus either increase or decrease specific activity.

Inhibitor sensitivity of xylanase variants

Analyzing the activity of the xylanase variants incubated with varying concentrations of inhibitor preparation revealed that their sensitivities to the xylanase inhibitor were significantly affected by the mutations. The variants N17Y, N29D, S31K, N32K, G120F, G120Y, D121N, T123D and Q175S all showed increased sensitivity to the inhibitor, compared with the BsX, where most other variants showed decreased sensitivity. Three xylanase variants (D11F, D11Y and D11K) were completely uninhibited by the xylanase inhibitor. The D11 residue appears to be essential to the interaction. However, other mutations in this residue (D11N, D11S and D11W) had less significant effect on the inhibitor sensitivity of the xylanase (Table I).

Projecting the highest observed reduction in inhibitor sensitivity of the mutations in each residue onto the structure of the BsX molecule indicates the relative importance of different areas of the BsX molecule surface for the interaction between BsX and the inhibitor protein (Figure 4).

Discussion

The influence of pH on the inhibition–xylanase interaction closely resembles the pH profile of enzyme activity. We see that as an indication of direct inhibitor–enzyme interaction within the active site of the enzyme. Tahir *et al*. (2004) have shown that a change of a single residue in the active site of AnX (D37A) abolishes interaction with both TAXI and XIP inhibitors, indicating that both inhibitors interact with the active site of the enzyme. For TAXI, this assumption has been confirmed by the published structure of the complex of

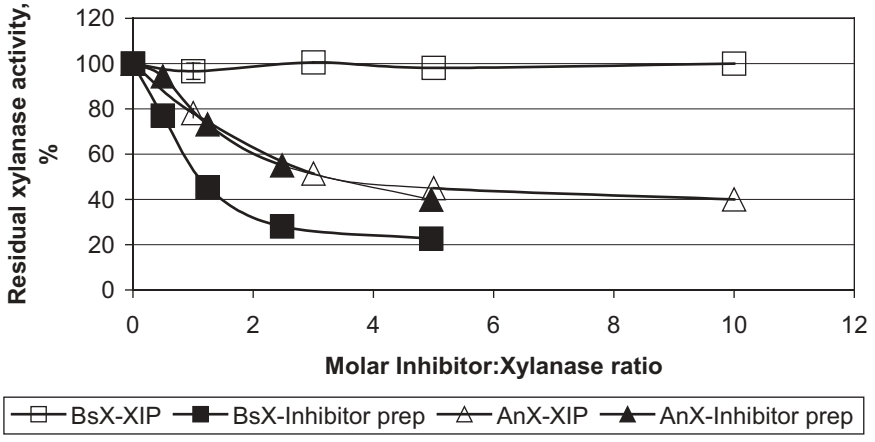

Fig. 2. Inhibition of BsX by pure XIP (BsX-XIP), BsX by inhibitor preparation containing both TAXI and XIP (BsX-inhibitor prep), AnX by pure XIP (AnX-XIP) and AnX by inhibitor preparation containing both TAXI and XIP (AnX-inhibitor prep).

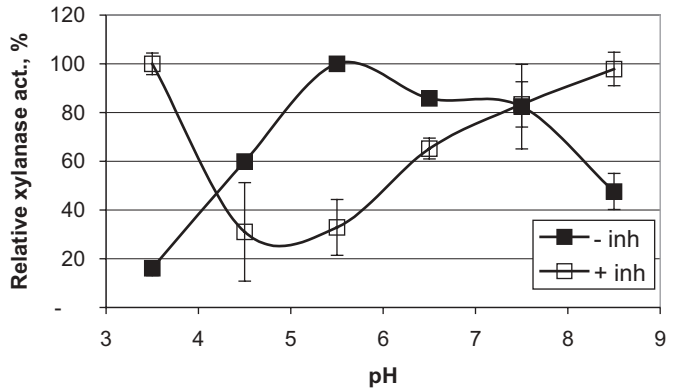

Fig. 3. pH optimum of BsX and the effect of pH on the interaction between BsX and inhibitor preparation (xylanase–TAXI molar ratio: 1 : 5).

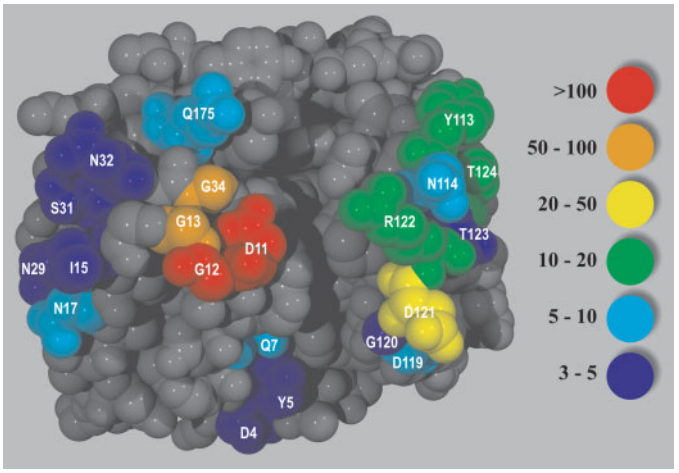

Fig. 4. Projection of the maximum obtained IC50 values of xylanase variants on the 3D structure of BsX. Residue colors represent ranges of the IC50 values of xylanase variants as indicated in the legend.

AnX and TAXI, where several residues of TAXI can be seen to mimic and take the position of xylose rings of a substrate bound to the enzyme (Sansen *et al.*, 2004b).

By choosing to work outside the active site, we expected to identify a range of amino acid residues, each contributing to the inhibitor interaction. The need to combine a subset of these in order to design a suitable, less inhibited enzyme was anticipated. Surprisingly, the variants produced, each comprising only a single mutation, form a set of enzymes with a large range of inhibition sensitivities from significantly increased sensitivity (N32K) compared with BsX, to completely abolish the interaction between the xylanase and the inhibitor (D11Y, D11F and D11K).

Residue D11 in BsX has no obvious counterpart in AnX as the N-termini of the two enzymes are the regions with the least sequence homology between the two molecules. They can be regarded as representatives of two subfamilies of the family 11 xylanases, but still they are both known to be inhibited by TAXI.

In our uninhibited D11 mutants (D11F, D11Y and D11K), we saw a reduction (74–86%) of the specific activity of the enzyme. The lack of binding to TAXI may therefore be due to sterical blocking, that also partially blocks the entrance of substrate to the active site. But we also saw the activity reduction in D11S, D11N and D11W mutants without seeing the same drastic effect on inhibitor binding. At least tryptophan should be able to provide sterical hindrance to the same extent as phenylalanine. The ranking of specific activity of the D11 variants (D11K<D11F<D11Y<D11W<D11N<D11S<D11) could indicate that the hydrogen bonding ability of the aspartic acid, which is strongly attached to the

Table I. Specific activity (XU/mg) and IC50 values of xylanase variants

Xylanase variants	XU/mg	IC50 (IU)
BsX	4162	3.8
D4A	3423	4.3
Y5A	3128	3.8
Q7A	2263	9.7
D11Y	1072	>>100
D11N	1344	7.8
D11L	0	ND
D11F	766	>>100
D11A	0	ND
D11K	563	>>100
D11S	1379	10.4
D11W	1133	15.6
G12F	3757	>100
G13F	4609	59.2
G14F	0	ND
I15K	4427	3.9
N17K	3656	4.3
N17Y	2889	3.3
N17D	1822	7.3
N29K	3298	4.1
N29Y	4058	4.2
N29D	4253	3.4
S31K	3991	3.4
S31Y	4193	4.0
S31D	3658	4.1
N32K	4152	3.2
G34D	1184	15.1
G34K	0	ND
G34F	2722	4.4
G34T	642	84.0
Q175E	3695	5.6
Q175S	2374	4.5
Q175L	5635	3.5
Y113A	4722	11.2
Y113D	5046	11.8
Y113S	0	ND
Y113K	3884	13.0
N114A	3135	3.9
N114D	4762	5.2
N114F	3572	5.3
N114K	2829	4.7
D119K	2188	6.0
D119Y	2202	4.1
D119N	1520	6.4
G120K	3813	4.2
G120D	4911	3.7
G120F	4348	2.7
G120Y	4873	3.1
G120N	4181	4.1
D121N	2857	2.9
D121K	2533	39.6
D121F	3321	19.6
D121A	2820	3.9
R122D	5461	5.4
R122F	4778	12.4
R122A	4787	4.0
R122T	0	ND
T123K	4504	3.9
T123Y	4211	3.9
T123D	4063	3.1
T124K	2402	19.3
T124Y	2478	8.2
T124D	3835	4.5

neighboring 'finger', is of importance for the activity and that substitution of D11 may cause some rearrangement in that area of the enzyme.

In the complex of TAXI and AnX (Sansen *et al*., 2004b) there appears to be no interaction between the N-terminal region of AnX and TAXI, indicating that this region is not important for the recognition or the binding between xylanase and TAXI. Overlaying a structure of BsX on AnX in the complex shows that residues 10–14 in BsX forms a loop that extends somewhat deeper into a cavity in TAXI, almost reaching the ceiling. Large residues in positions 11, 12 and 13 pointing outwards can hardly be accommodated, unless there is some mobility in that region. The cavity extends above BsX residues G34 and Q175 with a higher ceiling, in line with our observation that substitution of G34 with large residues has a less drastic effect on the interaction and that mutations in Q175 has only little effect. Substituting G34 with threonine may seem to have a surprisingly large effect on the interaction as threonine in this position does not appear to get in contact with the inhibitor. But the lowering of the specific activity by 85% could indicate that this substitution also causes a rearrangement that partially obstructs the active site entrance.

The remaining residues on the 'four fingers' (D4A, Y5A, Q7A, I15, N17, N29, S31 and N32) appear to be without direct interaction with TAXI, in agreement with the observed minor effect on inhibitor sensitivity.

In the thumb region of BsX (residues T109–Y128), our results indicate that Y113, D121, R122 and T124 interact directly with the inhibitor, whereas changes in residues N114 and D119 have less influence on the interaction. Changes in residues G120 and T123 have very limited influence on the inhibitor sensitivity and thus appear to be outside the area of direct contact. This is only partially confirmed by the structure of the AnX–TAXI complex, for example a side chain added to residue G120 would appear to clash with the inhibitor, whereas residue T124 appears to be outside the contact area as seen in the structure. But as the thumb region is flexible (Wakarchuk *et al*., 1994) and the whole region has to change position compared with that in the relaxed enzyme in order to bind to TAXI (Sansen *et al*., 2004b), then any imposed constraints to the flexibility of the thumb could also be influencing the enzyme–inhibitor interaction.

In conclusion, mutations on the surface of the molecule enzyme surrounding the active site cleft have a large effect on the interaction with TAXI. Though our data do not explain the exact mechanism behind the interaction between BsX and the wheat xylanase inhibitor, our strategy has proved to be highly efficient in developing novel uninhibited BsX-variants, having sufficiently high catalytic activity for industrial use.

Acknowledgements

We thank Dr Nathalie Juge, IFR, Norwich, UK for her kind gift of pure XIP-I. We thank Bente Sundgård and Helene Etzerodt for their excellent technical assistance.

References

Bedford,M. and Classen,H.L. (1992) In Visser,J., Beldman,G., Kusters van Someren,M.A. and Voragen,A.G.J. (eds) *Proceedings of an International Symposium*, pp 361–370.

Beliën,T., Van Campenhout,S., Van Acker,M. and Volkaert,G. (2005) *Biochem. Biophys. Res. Comm*., **327**, 407–414.

Brutus,A., Villard,C., Durand,A., Tahir,T., Furniss,C., Puigserver,A., Juge,N. and Giardina,T. (2004) *Biochim. Biophys. Acta*, **1701**, 121–128.

Campbell,R., Rose,D., Wakarchuk,W., To,R., Sung,W. and Yaguchi,M. (1993) In Suominen,P, and Reinikainen,T. (eds.), *Proceedings of the second TRICEL symposium on Trichoderma reesei cellulases and other hydrolases.* Foundation for Biotechnical and Industrial Fermentation Research, Helsinki, pp. 63–12.

Christophersen,C., Andersen,E., Jacobsen,T.S. and Wagner,P. (1997) *Starch/Stärke*, **49**, 5–12.

Collins,T., Gerday,C. and Feller,G. (2005) *FEMS Microbiol. Rev*., **29**, 3–23.

Corey,R.B. and Pauling,L. (1953) *Rev. Sci. Instr*., **24**, 621–627.

Courtin,C. and Delcour,J.A. (2002) *J. Cereal. Sci*., **35**, 225–243.

Coutinho,P.M. and Henrissat,B. (1999) Carbohydrate-Active Enzymes server at URL: http://afmb.cnrs-mrs.fr/CAZY/.

Debyser,W., Derdelinckx,G. and Delcour,J.A. (1997) *J. Am. Soc. Brew. Chem*., **55**, 153–156.

de Lemos Esteves,F., Ruelle,V., Lamotte-Brasseur,J., Quinting,B. and Frére,J.-M. (2004) *Protein Sci*., **13**, 1209–1218.

Flatman,R., McLauchlan,R., Juge,N., Furniss,C., Berrin,J.-G., Hughes,R.K., Manzanares,P., Ladbury,J.E., O'brian,R. and Williamson,G. (2002) *Biochem. J*., **365**, 773–781.

Fincher,G.B. and Stone,B.A. (1986) In Pomeranz,Y. (ed.), *Advances in Cereal Science and Technology*, Vol. 8. AACC, St. Paul, MN, pp. 207–295.

Furniss,C.S.M., Belshaw,N.J., Alcocer,M.J.C., Williamson,G., Elliott,G.O., Gebruers,K., Haigh,N.P., Fish,N.M. and Kroon,P.A. (2002) *Biochem. Biophys. Acta*, **1598**, 24–29.

Gasteiger,E., Gattiker,A., Hoogland,C., Ivanyi,I., Appel,R.D. and Bairoch,A. (2003) *Nucleic Acids Res*., **31**, 3784–3788.

Gebruers,K., Debyser,W., Goesaert,H., Van Campenhout,S. and Delcour,J.A. (2001) *Biochem. J*., **353**, 239–244.

Gebruers,K. *et al*. (2004a) *Biochem. Biophys. Acta*, **1696**, 213–221.

Gebruers,K., Fierens,E., Rombouts,S., Courtin,C.M., Brijs,K., Volckaert,G., Van Campenhout,S. and Delcour,J.A. (2004b) Abstract from the AACC Annual Meeting, September 2004, San Diego, CA.

Henrissat,B. (1991) *Biochem. J*., **280**, 309–316.

Joshi,M.D., Sidhu,G., Pot,I., Brayer,G.D., Withers,S.G. and McIntosh,L.P. (2000) *J. Mol. Biol*., **299**, 255–279.

Juge,N., Payan,F. and Williamson,G. (2004) *Biochem. Biophys. Acta*, **1696**, 203–211.

Koltun,W.L. (1965) *Biopolymers*, **3**, 665–679.

Liu,L., Li,X., Li,X. and Shao,W. (2004) *Biochem. Biophys. Res. Commun*., **321**, 391–396.

Maat,J. *et al*. (1992) In Visser,J., Beldman,G., Kusters van Someren,M.A. and Voragen,A.G.J. (eds.) *Proceedings of an International Symposium*, pp. 349–360.

McLauchlan,R., Garcia-Conesa,M.T., Williamson,G., Roza,M., Ravestein,P. and MacGregor,A.W. (1999) *Biochem. J*., **338**, 441–446.

Moreau,A., Shareck,F., Kluepfel,D. and Morosoli,R. (1994) *Enzyme Microb. Technol*., **16**, 420–424.

Paice,M.G., Bourbonnais,R., Desrochers,M., Jurasek,L. and Yaguchi,M. (1986) *Arch. Microbiol*., **144**, 201–206.

Payan,F. *et al*. (2004) *J. Biol. Chem*., **279**, 36029–36037.

Ponyi,T., Szabó,L., Nagy,T., Orosz,L., Simpson,P.J., Williamson,M.P. and Gilbert,H.J. (2000) *Biochemistry*, **39**, 985–991.

Rouau,X. and Surget,A. (1998) *J. Cereal Sci.*, **28**, 63–70.

Rouau,X., El-Hayek,M.-L. and Moreau,D. (1994) *J. Cereal Sci.*, **19**, 259–272.

Sansen,S., De Ranter,C.J., Gebruers,K., Brijs,K., Courtin,C.M., Delcour,J.A. and Rabijns,A. (2004a) *Acta Crystallogr. D Biol. Crystallogr.*, **60**, 555–557.

Sansen,S., De Ranter,C.J., Gebruers,K., Brijs,K., Courtin,C.M., Delcour,J.A. and Rabijns,A. (2004b) *J. Biol. Chem.*, **279**, 36022–36028.

Sibbesen,O. and Sørensen,J.F. (1998) Patent application WO 00/39289.

Sibbesen,O. and Sørensen,J.F. (2001) Patent application WO 01/66711.

Tahir,T.A., Berrin,J.-G., Flatman,R., Roussel,A., Reopstorff,P., Williamson,G. and Juge,N. (2002) *J. Biol. Chem*., **15**, 44035–44043.

Tahir,T.A., Durand,A., Gebruers,K., Roussel,A., Wiliamson,G. and Juge,N. (2004) *FEMS Microbiol. Lett.*, **239**, 9–15.

Viikari,L., Ranva,M., Kantelinen,A., Sandquist,J. and Linko,M. (1986) In *Third International Conference in Biotechnology in Pulp and Paper Industry*, pp. 67–69.

Wakarchuk,W.W., Campbell,R.L., Sung,W.L., Davoodi,J. and Yaguchi,M. (1994) *Protein Sci*., **3**, 467–475.

Whistler,R. and Masek,E. (1955) *J. Am. Chem. Soc.*, **77**, 1241–1243.

Received August 23, 2005; revised January 25, 2006; accepted January 26, 2006

Edited by Anthony Wilkinson